doi:10.1093/brain/awv289 BRAIN 2015: 138; 3581–3597 | 3581

BRAIN
A JOURNAL OF NEUROLOGY

Retinoid X receptor activation reverses age-related deficiencies in myelin debris phagocytosis and remyelination

Muktha S. Natrajan,[1,2] Alerie G. de la Fuente,[1] Abbe H. Crawford,[1] Eimear Linehan,[3] Vanessa Nuñez,[4] Kory R. Johnson,[2] Tianxia Wu,[2] Denise C. Fitzgerald,[3] Mercedes Ricote,[4] Bibiana Bielekova[2] and Robin J. M. Franklin[1]

The efficiency of central nervous system remyelination declines with age. This is in part due to an age-associated decline in the phagocytic removal of myelin debris, which contains inhibitors of oligodendrocyte progenitor cell differentiation. In this study, we show that expression of genes involved in the retinoid X receptor pathway are decreased with ageing in both myelin-phagocytosing human monocytes and mouse macrophages using a combination of *in vivo* and *in vitro* approaches. Disruption of retinoid X receptor function in young macrophages, using the antagonist HX531, mimics ageing by reducing myelin debris uptake. Macrophage-specific RXRα (*Rxra*) knockout mice revealed that loss of function in young mice caused delayed myelin debris uptake and slowed remyelination after experimentally-induced demyelination. Alternatively, retinoid X receptor agonists partially restored myelin debris phagocytosis in aged macrophages. The agonist bexarotene, when used in concentrations achievable in human subjects, caused a reversion of the gene expression profile in multiple sclerosis patient monocytes to a more youthful profile and enhanced myelin debris phagocytosis by patient cells. These results reveal the retinoid X receptor pathway as a positive regulator of myelin debris clearance and a key player in the age-related decline in remyelination that may be targeted by available or newly-developed therapeutics.

1 Wellcome Trust-MRC Cambridge Stem Cell Institute, and Department of Clinical Neurosciences, University of Cambridge, Cambridge, CB2 0AH, UK
2 Neuroimmunological Diseases Unit, National Institute of Neurological Disorders and Stroke, National Institutes of Health, Bethesda, MD, USA
3 Centre for Infection and Immunity, Queen's University Belfast, UK
4 Department of Cardiovascular Development and Repair, Centro Nacional de Investigaciones Cardiovasculares Carlos III (CNIC), Madrid, Spain

Correspondence to: Prof. Robin Franklin,
Wellcome Trust-MRC Cambridge Stem Cell Institute,
The Clifford Allbutt Building,
Cambridge Biomedical Campus,
University of Cambridge,
Hills Road,
Cambridge CB2 0AH,
UK
E-mail: rjf1000@cam.ac.uk

Correspondence may also be addressed to: Dr Bibiana Bielekova, Neuroimmunological Diseases Unit, National Institute of Neurological Disorders and Stroke, National Institutes of Health, Bethesda, MD 20892, USA
E-mail address: Bibi.Bielekova@nih.gov

Received April 8, 2015. Revised August 10, 2015. Accepted August 14, 2015. Advance Access publication October 13, 2015

Keywords: remyelination; ageing; retinoid X receptor; myelin debris; monocyte-derived macrophages

Abbreviations: 9cRA = 9-*cis* retinoic acid; RXR = retinoid X receptor

Introduction

CNS remyelination is a regenerative process that can restore function and prevent axonal degeneration in chronic demyelinating diseases such as multiple sclerosis (Franklin and ffrench-Constant, 2008; Franklin and Gallo, 2014). It occurs when adult oligodendrocyte progenitor cells respond to demyelination by activation, proliferation, migration and finally differentiation into new myelin-forming oligodendrocytes (Levine and Reynolds, 1999; Zawadzka *et al.*, 2010; Moyon *et al.*, 2015). As with all regenerative processes, the rate of remyelination declines progressively with adult ageing (Sim *et al.*, 2002; Goldschmidt *et al.*, 2009). Several lines of evidence indicate that this is largely the result of an age-associated impairment of oligodendrocyte progenitor cell differentiation due to both environmental factors and cell-intrinsic mechanisms that change with ageing (Chari *et al.*, 2003; Woodruff *et al.*, 2004; Shen *et al.*, 2008).

A key environmental factor regulating oligodendrocyte progenitor cell differentiation during remyelination is the fate of the myelin debris generated during demyelination (Kotter *et al.*, 2006; Neumann *et al.*, 2009). Myelin debris contains inhibitors of oligodendrocyte progenitor cell differentiation and thus its clearance by phagocytic macrophages, derived from both microglia and from monocytes recruited from the circulation, is an important component of creating a lesion environment in which oligodendrocyte progenitor cells can differentiate into remyelinating oligodendrocytes. The efficiency of myelin debris clearance declines with ageing, contributing to the delayed differentiation of oligodendrocyte progenitor cells and age-associated decline in remyelination efficiency (Shields *et al.*, 1999; Ruckh *et al.*, 2012; Linehan *et al.*, 2014). Therefore, understanding the mechanisms underpinning the age-related decline in myelin debris phagocytosis is important for devising means by which the decline in remyelination might be therapeutically reversed. The aim of this study was to determine the functional and molecular differences between young and older adult microglia- and monocyte-derived macrophages involved in myelin debris phagocytosis, and to identify therapeutically modifiable pathways associated with efficient myelin debris clearance.

Materials and methods

Animals

Female C57Bl/6 mice were used for *in vitro* cell isolations. LysMCre^{+} RXRα$^{fl/fl}$ knockout mice were generated at the CNIC Madrid as previously described (Núñez *et al.*, 2010). Mice with floxed RXRα alleles were crossed with LysMCre^{+} mice to create macrophage-specific RXRα knockouts. Mice with lox-P-targeted RXRα and the LysMCre transgene were crossed with RXRα floxed mice to obtain knockouts (LysMCre^{+}RXRα$^{fl/fl}$) and wild-types (LysMCre^{-}RXRα$^{fl/fl}$). All experiments were performed under the UK Home Office project license.

Myelin isolation

Brains were removed from adult mice, and myelin was isolated using a discontinuous sucrose gradient as previously described (Kotter *et al.*, 2006). Briefly, brains were homogenized in ice-cold 0.32 M sucrose and homogenate was laid over 0.85 M sucrose solution. Suspensions were subjected to ultracentrifugation (100 000*g*, 4°C, 1 h) and interfaces were washed (55 000*g*, 4°C, 10 mins). Pellets were resuspended in phosphate-buffered saline (PBS) and stored at −80°C. Prior to each flow cytometry assay, the required amount of myelin debris was fluorescently labelled using the lipophilic dyes pkh26 or $DiOC_{18}(3)$ (DiO) (Sigma).

Peritoneal macrophages and microglia

Peritoneal macrophages were harvested by peritoneal lavage with 10 ml of cold PBS. Peritoneal macrophages were plated in Dulbecco's modified Eagle medium supplemented with foetal bovine serum (FBS, 10%), L-glutamine (2 mM) and penicillin/streptomycin. For microglia, a CNS tissue suspension was prepared using the Neural Tissue Dissociation Kit (Miltenyi Biotec). Myelin debris was removed using Myelin Removal Beads II (Miltenyi Biotec). Microglia were then isolated using CD11b^{+} selection (Miltenyi Biotec). Peritoneal macrophages and microglia were seeded on chamber slides (7×10^4/well) for immunocytochemistry or 96-well plates for flow cytometry. Fluorescently labelled myelin (10 μg/ml protein) was added for 2 h. Cells for flow cytometry were incubated with anti-CD16/CD32 (eBioscience, 14-0161-81), stained with anti-CD11b and anti-CD45 (eBioscience, 48-0112) and fixed with Medium A (Invitrogen) prior to acquisition on a BD FACSCanto II. Chamber slides were fixed with 4% paraformaldehyde (PFA) then washed and blocked with 10% normal goat serum. Cells were stained with CD11b, washed and stained with DAPI. Finally, slides were visualized with a Leica DM5500 microscope using a Leica DFC340 FX camera.

Bone marrow monocyte-derived macrophages

Bone marrow was flushed from the femurs/tibiae of mice. Bone marrow cells were cultured for 7 days in RPMI1640 with FBS (10%), L-glutamine (2 mM), penicillin/streptomycin, and 20% L929 conditioned media (to provide macrophage colony stimulating factor for differentiation). On Day 7, macrophages

were placed into macrophage serum-free media (Gibco) overnight before beginning experiments. All experiments were carried out in serum-free media, with treatments described in the Supplementary material.

Western blots

Bone marrow monocyte-derived macrophages were lysed with 10% sucrose with Halt protease/phosphatase inhibitor (ThermoScientific) and homogenized. Five to 15 µg of sample were loaded in Bis-Tris gels (Invitrogen). Gels were run at 100 V for 2 h 30 min in MOPS sodium dodecyl sulphate running buffer and transferred onto nitrocellulose membranes (GE Healthcare) and blocked with 5% milk in PBS-Tween for 1 h. The primary RXRα antibody (Santa Cruz, 1:100, sc-553) was incubated overnight at 4°C then washed with PBS-T. Horseradish peroxidase-conjugated goat anti-rabbit secondary (Dako, 1:1000, P0448) was added for 2 h. Proteins were detected with ECL (Amersham). Membranes were further incubated with β-actin (Sigma, 1:20 000, A5441) followed by goat anti-mouse secondary (Dako, 1:1000, P0447), and films were developed and quantified with ImageJ and normalized using the correspondent β-actin band.

Flow cytometry for bone marrow monocyte-derived macrophages

Media were changed on bone marrow monocyte-derived macrophages and HX531 or dimethyl sulphoxide controls were added for 24 h. Subsequently, DiO-labelled myelin (30 µg/ml) was added to phagocytosing groups for 8 h. Cells were then washed, detached, and centrifuged at 300 *g* for 5 min. Pellets were resuspended in FACS buffer (PBS, 1% FBS), and CD11b-APC (Miltenyi, 1:100, 130-098-088) was added for 30 min at 4°C. Cells were then washed and resuspended in FACS buffer and acquired on a BD FACSCalibur. Phagocytosis index was equal to the percentage of myelin$^+$CD11b$^+$ double-positive cells.

Immunocytochemistry

Bone marrow monocyte-derived macrophages were replated to 24-well plates at 10^5/well on glass coverslips overnight. Media (Gibco) were changed, and treatments were added for 24 h. Myelin debris (30 µg/ml) was then added to phagocytosing groups for 8 h. Cells were fixed in 4% PFA, washed, then coverslips were blocked in 5% normal goat serum (Sigma) with 0.1% Triton™ X-100 for 1 h. Primary antibodies (Iba1: Wako, 1:500, 019-19741; CD11b: Serotec, 1:250, MCA711; RXRα: SantaCruz, 1:100, sc-553; Anti-MBP: Serotec, 1:500, MAC409S) were diluted in blocking solution and added for 1 h. Secondary antibodies were applied for 1 h at 1:500 (Invitrogen: goat 488 anti-rabbit, A11034; goat 568 anti-rat, A11077; goat 568 anti-rabbit, A11036). Cell nuclei were stained 5 min with Hoechst (Biotium, 40043) and mounted and visualized using a Zeiss Axiovision Observer A1AX10 or Leica Confocal microscope. Cells were counted using ImageJ. Phagocytosis index was calculated by: percentage myelin-laden macrophages = (MBP$^+$ myelin-containing macrophages)/(total *n* of Iba1$^+$ macrophages).

Lysolecithin-induced focal demyelination

Demyelinating lesions were induced in the ventral funiculus of the thoracic spinal cord of LysMCre$^+$RXRα$^{fl/fl}$ and LysMCre$^-$RXRα$^{fl/fl}$ mice on C57Bl/6 background with 1 µl 1% lysolecithin. Mice were intracardially perfused with 4% glutaraldehyde or 4% PFA at 5 , 14 , and 21 days post lesion. These time points represent significant events in remyelination: 5 days post lesion = oligodendrocyte progenitor cell recruitment and proliferation; 14 days post lesion = oligodendrocyte progenitor cell differentiation; 21 days post lesion = complete remyelination. PFA-fixed spinal cords were post-fixed in sucrose before O.C.T. embedding (Tissue-Tech) and storage at −80°C. OCT-embedded tissue was cut in 12-µm segments using a Leica Cryostat Microtome and stored at −80°C prior to staining.

Oil Red O staining

Tissue sections were dried in 100% propylene glycol then stained at 60°C in 0.5% Oil Red O solution (Sigma) for 6 min. Slides were switched to 85% propylene glycol for 2 min followed by rinsing. Nuclei were stained with haematoxylin (Sigma) for 1 min and washed. Slides were mounted and visualized with a Nikon Eclipse E600 microscope. Area of staining was quantified using ImageJ.

Immunohistochemistry

Frozen sections were permeabilized and blocked with PBS containing 5% normal goat serum and 0.3% Triton™ X-100 for 1 h. For nuclear antibodies, Antigen Retrieval Buffer (1:10, Dako) was preheated to 95°C and slides were incubated at 75°C for 10 min. Slides were then washed, and primary antibodies were applied overnight at 4°C (Mouse CC1: Calbiochem, 1:100, OP80; Rabbit OLIG2: Millipore, 1:1000, AB9610). Sections were washed and incubated with fluorescently conjugated secondary antibodies (Invitrogen) for 2 h. Slides were visualized using a Zeiss Axiovision Observer A1 microscope.

In situ hybridization

Proteolipid protein probe was prepared and diluted in hybridization buffer and *in situ* hybridization was performed as previously described (Fancy *et al.*, 2004), and further described in the Supplementary material.

Electron microscopy

Glutaraldehyde-perfused spinal cords were post-fixed and visualized with a transmission electron microscope, further described in the Supplementary material. The g-ratio was used for extent of remyelination on axons. G-ratio = (axon diameter) / (axon + outer myelin diameter).

Human subjects

Studies were performed according to US National Institutes of Health guidelines and all subjects signed informed consent.

Study subjects were healthy volunteers in two age groups, Young ($\leqslant$35 years old) and Old ($\geqslant$55 years old), and patients with multiple sclerosis diagnosed at the NIH based on the 2010 revisions of the McDonald diagnostic criteria.

Human monocyte isolation and treatment

Peripheral blood mononuclear cells were isolated from whole blood using lymphocyte separation medium (Lonza). $CD14^+$ monocytes were isolated by positive selection (MACS Miltenyi) and plated in 6-well plates at 10^6/well (for RNA) or in suspension in 96-well plates at 10^5/well (for flow cytometry) in X-VIVO™ without phenol red (Lonza). Bexarotene (Sigma) was used to activate retinoid X receptors (RXRs). To calculate the concentration to use *in vitro*, we considered the concentration achieved in the serum of patients on the FDA-approved dose of 300 mg/m^2/day, with a C_{max} plasma of 911 µg/l in patients or ~2 µM (Lowe and Plosker, 2000). Therefore, we chose the *in vivo* achievable dose of 1 µM.

Myelin isolation

Brain tissue from a post-mortem primary progressive multiple sclerosis patient was used for myelin isolation. Myelin was isolated and stored as in mice (see above). For flow cytometry, myelin was labelled with pHrodo® Green STP Ester (Invitrogen) and stored at −20°C in the dark.

Microarrays and quantitative polymerase chain reaction arrays

Monocytes were separated in 6-well plates for two separate microarrays. The first data set, comparing Young healthy volunteers and Old healthy volunteers, compared two groups per donor: Control cells (no treatment) and Phagocytosing cells (treated with myelin, 10 µg/ml). For the second data set, two donor groups (Young healthy volunteers and all multiple sclerosis patients) with three groups per donor were used: Control cells (no treatment), Phagocytosing cells (treated with myelin, 10 µg/ml), and Bexarotene-treated Phagocytosing cells. Cells were then collected in TRIzol® (Invitrogen) and stored at −80°C. RNA was isolated using miRNeasy kit (Qiagen) with $n \geqslant 3$ per age group. RNA concentration was measured using a NanoDrop ND-1000 and processed at the NIH Microarray Core Facility on Affymetrix 1.0 ST Human Gene Arrays. Microarrays and retinoic acid quantitative polymerase chain reaction (PCR) arrays are further described in the Supplementary material.

Flow cytometry

Monocytes in 96-well plates were incubated with 1 µM bexarotene (treated groups) for 1 h at 37°C. Cells were then stained with CD14-APC (eBioscience, 17-0149) for 10 min at 37°C. Cells were washed in FACS buffer by centrifuging at 250 *g*, 5 min, 4°C and resuspended in warm X-VIVO without phenol red (Lonza). pHrodo®-labelled myelin was added to phagocytosing groups for 20 min at 37°C. Cold FACS buffer was then added with cells immediately acquired on a BD LSR II and analysed with BD FACSDiva 6.1. Gating was based on non-phagocytosing controls. Phagocytosis index was calculated by: (mean fluorescent intensity of $FITC^+$ myelin-phagocytosing monocytes) / (mean fluorescent intensity of $FITC^+$ non-phagocytosing monocytes).

Statistical analysis

Mouse experiments

Data are presented by mean ± standard error of the mean (SEM) in all graphs. Statistical analysis was done using Excel 2010 and Graphpad Prism 6. When comparing more than two groups with only one independent variable, one-way ANOVA was used followed by Tukey's multiple comparisons test. When two or more variables were involved, a two-way ANOVA was used, and if interaction was positive, further analysis was done by Sidak's multiple comparisons test considering these variables separately. Two-tailed unpaired Student's *t*-tests were used when comparing two normally distributed groups. Results were considered significant if $P < 0.05$. Technical replicates were performed $n \geqslant 3$/experiment, with $n \geqslant 4$ biological replicates (animals) per experiment.

Human experiments

Power analysis was conducted in nQuery using an internal pilot study including 18 young and 17 old healthy volunteers with outcomes from pretreatment, and 48 multiple sclerosis patients with outcome from both pre- and post-treatment. Based on a significance level of 0.05, a sample size of 18 subjects was required to have 80% power for detecting the difference between pre and post-treatment using a paired *t*-test; a sample size of 34 subjects per group was required to have 80% power for detecting the difference between the young and old healthy volunteer groups using a two-sample *t*-test. Two-way repeated measures ANOVA was performed to evaluate the effect of group and treatment, and the interaction between group and treatment. When the interaction was significant, pairwise comparisons were conducted with Tukey's correction procedure. Natural logarithm was applied to the outcome since the distribution had a long right tail. SAS 9.2 and Graphpad Prism were used for the statistical analysis and $P < 0.05$ was used as the significance level.

Results

Ageing impairs myelin debris phagocytosis

Previous studies have revealed an age-associated decline in myelin debris clearance following experimental induction of primary demyelination (Shields *et al.*, 1999; Ruckh *et al.*, 2012). To test whether this occurs because of an age-associated decline in the intrinsic function of cells primarily responsible for myelin debris clearance, we examined the effects of ageing on phagocytosis in several types of macrophages. Phagocytosis was assessed either by counting the number of macrophages containing labelled myelin and dividing by the total number of macrophages or by

determining the percentage of cells staining positive for both macrophage and myelin markers by flow cytometry. Purified peritoneal macrophages from young (2-month-old) mice incubated with fluorescently-labelled myelin fragments were more efficient at myelin phagocytosis than peritoneal macrophages from old (15–20-month-old) mice (Fig. 1A–C). Bone marrow monocyte-derived macrophages also showed an age-dependent decrease in myelin phagocytosis, although the phagocytic ability of these cells was not significantly affected until mice reached 24 months old (Fig. 1D and E, young = 2 months old, old = 24 months old). As microglia-derived macrophages are also likely to be involved in myelin debris clearance (Yamasaki *et al.*, 2014; Lampron *et al.*, 2015), we next determined whether microglia are similarly affected by ageing (Fig. 1F and G, young = 2 months old, old = 15–20 months old). Microglia were less efficient at myelin phagocytosis than other macrophage types; only 19% of young microglial cells ingested myelin debris compared to 50–70% phagocytosis in other young tissue-derived macrophages. However, again, ageing significantly impaired myelin phagocytosis by microglia (Fig. 1H).

Transcriptional profiling reveals changes in RXR associated with the decline in myelin phagocytosis

We next asked whether defects in myelin phagocytosis observed in ageing animals are also present in ageing humans. We used blood-derived monocytes isolated from healthy volunteers as these could be readily obtained in large numbers for functional studies. We provided pilot myelin–phagocytosis data to the statistician for calculating the sample size needed for functional comparison of monocytes derived from young ($\leqslant$35 years old) and old ($\geqslant$55 years old) healthy volunteers. Fluorescently-labelled myelin debris phagocytosis was determined by comparing $FITC^+$ fluorescence in phagocytosing cells with control cells. The phagocytosis index was calculated by mean fluorescence of myelin-phagocytosing cells divided by that of resting cells. This method accounts for background levels of $FITC^+$ fluorescence in different samples and compares exact levels of fluorescence, which are more comparable across several days/runs needed when collecting human samples (Schreiner *et al.*, 2011). Upon acquiring predetermined sample sizes ($n = 34$ for each group), we observed a modest, but highly significant decrease in the efficiency of myelin phagocytosis by monocytes derived from old healthy volunteers (Fig. 2A–C).

To identify possible mechanisms involved in the age-associated changes in phagocytic cells responsible for myelin debris clearance, we undertook gene expression profiling. We argued that human experiments might provide more general data, due to genetic heterogeneity among human subjects, with direct relevance to patients, whose mechanisms could be explored subsequently using animal models. Microarrays were performed on myelin-phagocytosing monocytes from young and old healthy volunteers and showed that myelin phagocytosis caused a strong shared change in the expression profiles (i.e. 70% of changed genes), while fewer phagocytosis-induced changes were specific for monocytes derived from young (15% of changed genes) versus old (i.e. 15% of changed genes) healthy volunteers (Supplementary Fig. 1A–D). Therefore, to define the mechanistic pathways enriched in monocytes on phagocytosis and provide evidence for the cause of the functional decline with age, we used Ingenuity Pathway Analysis to determine the canonical pathways affected by the 1102 (30%) genes differentially regulated upon phagocytosis in young and old monocytes (Supplementary Fig. 1E). This analysis revealed that the RXR pathway was differentially regulated. RXRs are nuclear receptors that act both homodimerically and heterodimerically as ligand-activated transcription factors. In young cells, RXR heterodimer pathways were significantly upregulated ($P < 0.05$), with 13 positive regulators upregulated and seven downregulated, while these pathways were downregulated in old cells, with five upregulated and 14 downregulated (Supplementary Table 1). Several RXR binding partners and downstream target genes were plotted with Ingenuity Pathway Analysis, and the genes identified in the microarray of young cells showed mostly upregulation of positive regulators of RXR, including transcriptional targets, binding partners, and regulators of RXR (Fig. 2D), while the profile of old cells showed mostly downregulation of genes related to this pathway (Fig. 2E).

To confirm the results from the microarray in an independent cohort, quantitative real-time PCR was performed with a Retinoic Acid Signaling PCR Array (SABiosciences). After monocytes were exposed to myelin debris, cells were collected and relative gene expression was determined in groups of pooled young or old myelin-phagocytosing cells compared to young controls. The PCR arrays confirmed the results seen in the microarray, with the RXR pathway more highly upregulated upon myelin phagocytosis in young monocytes (Fig. 2F). The quantitative PCR revealed that both RXRα (encoded by *RXRA*) and RXRβ (*RXRB*) as well as binding partners of RXR, such as RAR (*RARA*) and PPAR (*PPARA*), are downregulated in aged myelin-phagocytosing monocytes.

The RXR agonist 9-*cis* retinoic acid enhances myelin phagocytosis in aged macrophages

We next asked whether the age-associated defects in RXR pathways in phagocytosing cells have *in vivo* consequences for remyelination by testing the hypothesis that RXR signalling is involved in the delayed myelin clearance that limits efficient remyelination with ageing. To do this, we reverted to animal models where the hypothesis could be tested experimentally.

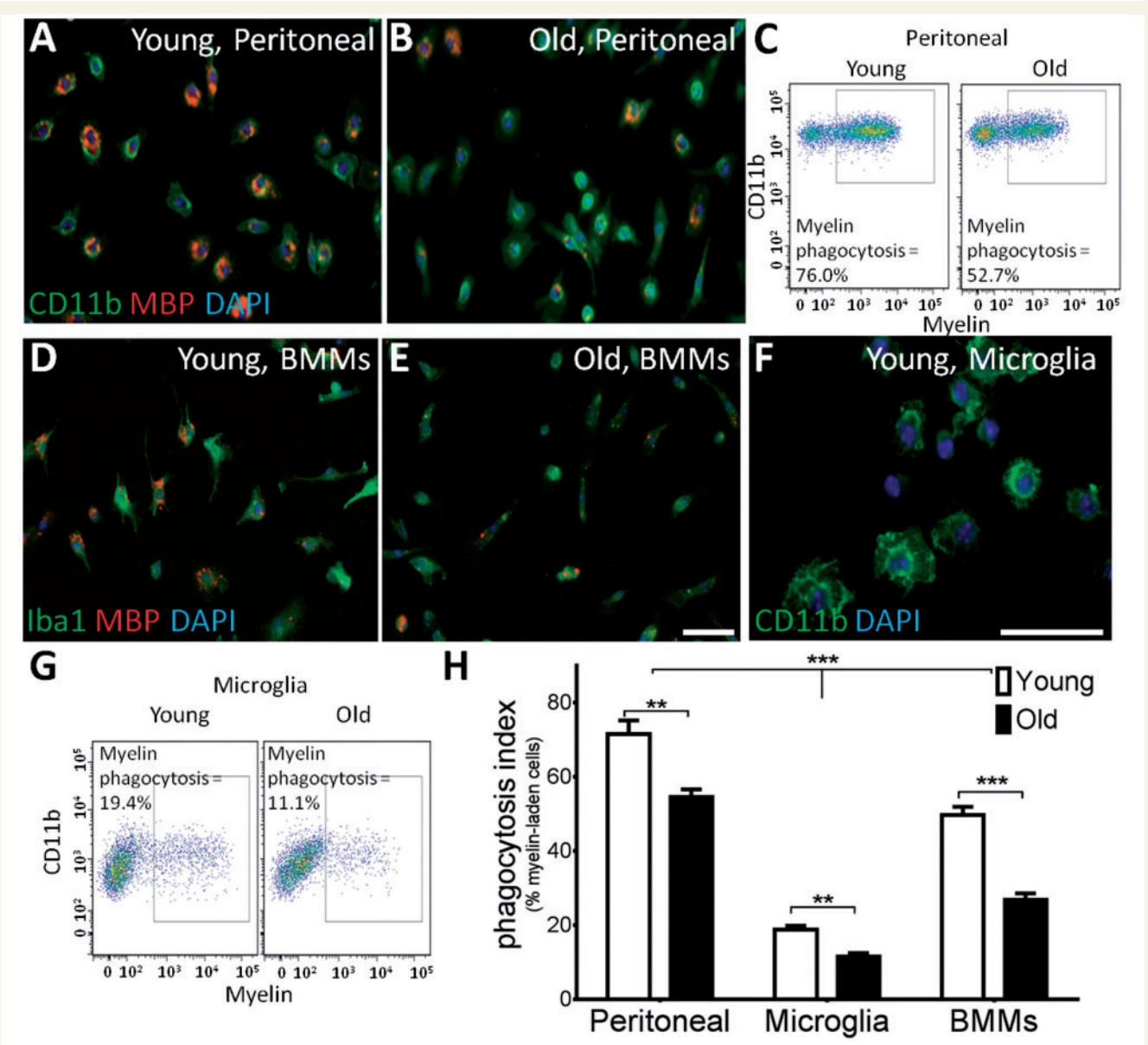

Figure 1 Ageing impairs myelin debris phagocytosis. Macrophage cultures were incubated with fluorescent myelin and phagocytosis was analysed. (**A–C**) Aged peritoneal macrophages were visualized by immunocytochemistry (**A** and **B**) and showed impairment in myelin phagocytosis by flow cytometry (**C**). (**D** and **E**) Bone marrow monocyte-derived macrophages (BMMs) showed a decrease in myelin debris phagocytosis with age. (**F** and **G**) Myelin debris uptake is reduced in microglia cultures from aged mice compared to young. (**H**) All three macrophage subtypes showed significantly reduced myelin debris phagocytosis with age. There were significantly fewer myelin-phagocytosing microglia compared to peritoneal macrophages or bone marrow monocyte-derived macrophages regardless of age. Young = 2-month-old mice, Old = 15–24-month-old mice. Phagocytosis index = % MBP^+ Iba^+ cells. Scale bars = 50 μm. Two-way ANOVA and *post hoc* Sidak's multiple comparisons test, Mean ± SEM, $^{**}P < 0.01$, $^{***}P < 0.001$, n = 4/age group.

As many genes in the RXR pathway were downregulated with age, we first assessed the levels of protein expression of this receptor family. Of the three isoforms of RXR, RXRα has the highest expression in monocytes and macrophages, whereas RXRβ is expressed to a lesser extent (Roszer *et al.*, 2013). RXRα expression in myelin-phagocytosing macrophages was confirmed using immunocytochemical staining and confocal imaging of $Iba1^+$ bone marrow monocyte-derived macrophages with RXRα found to be localized to the nucleus (Fig. 3A). Using western blots, we determined the protein expression of RXRα in ageing myelin-phagocytosing mouse bone marrow monocyte-derived macrophages compared to β-actin controls. The RXRα band has a weight of 55 kD with another non-specific band indicated on the gel (Fig. 3B); this distribution of bands has also been seen in previous studies (Kuhla *et al.*, 2011; Menéndez-Gutiérrez *et al.*, 2015). By isolating bone marrow monocyte-derived macrophages

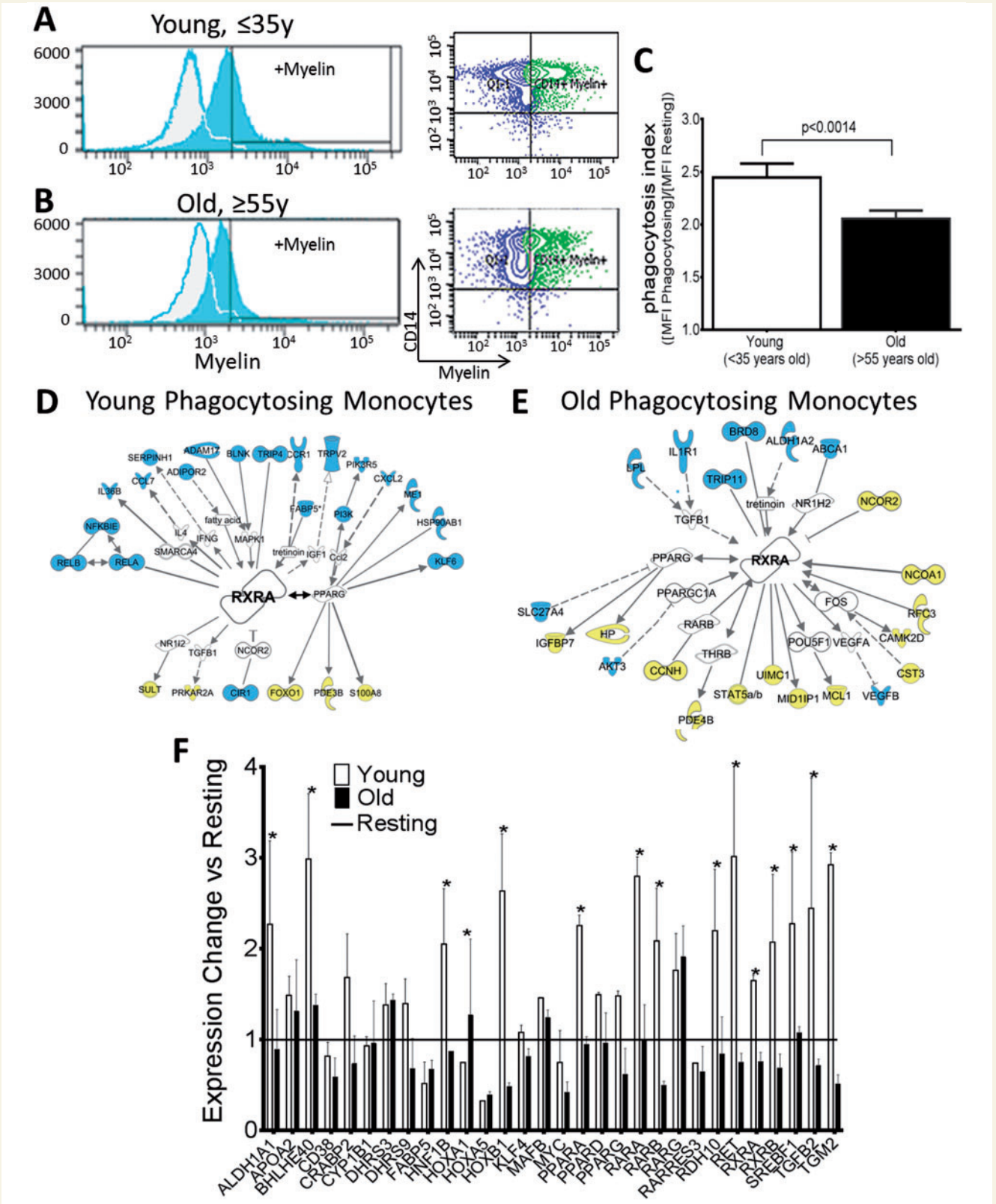

Figure 2 Myelin debris phagocytosis is reduced and RXR pathways are downregulated in aged myelin-phagocytosing monocytes. (**A**) Monocytes from healthy volunteers (⩽35 years old) effectively phagocytose myelin debris (Phagocytosis index = 2.44 ± 0.06). Myelin + gate was determined by non-phagocytosing control cells (grey background plots). (**B** and **C**) Monocytes from aged volunteers (⩾55 years old) show significantly impaired myelin debris uptake (2.05 ± 0.04). Adjusted *P*-values for pairwise comparisons in a two-way repeated measures ANOVA with Tukey's procedure based on log-transformed outcomes, mean ± SEM, $P = 0.0014$, $n = 36$/group. Statistical analysis was performed on the full dataset represented in Fig. 7C. Phagocytosis index = (mean fluorescent intensity of myelin-phagocytosing monocytes / mean

(continued)

from mice of different ages, we were able to correlate the change in RXRα expression with ageing. In young, 2-month-old macrophages, RXRα expression was highest. The levels of RXRα protein in adult mice decreased with age and reached statistical significance ($*P < 0.05$) when comparing expression in 2-month-old mice to the oldest age group of 24 months old (Fig. 3C).

There are several synthetic ligands for RXR, and one of the most widely used high-affinity ligands is 9-*cis* retinoic acid (9cRA) (Heyman *et al.*, 1992). Here, we added 1μM 9cRA to myelin-phagocytosing bone marrow monocyte-derived macrophages to activate RXR *in vitro*. Macrophages were labelled with the myeloid marker Iba1 and ingested myelin was labelled with myelin basic protein (MBP). Young (2-month-old) controls were able to effectively clear myelin, and the addition of 9cRA did not augment phagocytosis (Fig. 4A and B). However, old (32-month-old) macrophages showed significantly reduced myelin debris clearance (Fig. 4C) compared to young. When RXR was activated by 9cRA, significantly more old bone marrow monocyte-derived macrophages were able to phagocytose debris (Fig. 4D and E). There was still a significant difference between 2-month-old and 32-month-old + 9cRA treated cells, indicating that RXR activation cannot restore phagocytic ability completely, but the addition of 9cRA has the potential to enhance debris clearance in aged animals.

Loss of RXR function in young macrophages impairs myelin debris clearance and delays remyelination

As there was no significant difference when 9cRA was added to 2-month-old bone marrow monocyte-derived macrophages, we hypothesized that ligand-independent,

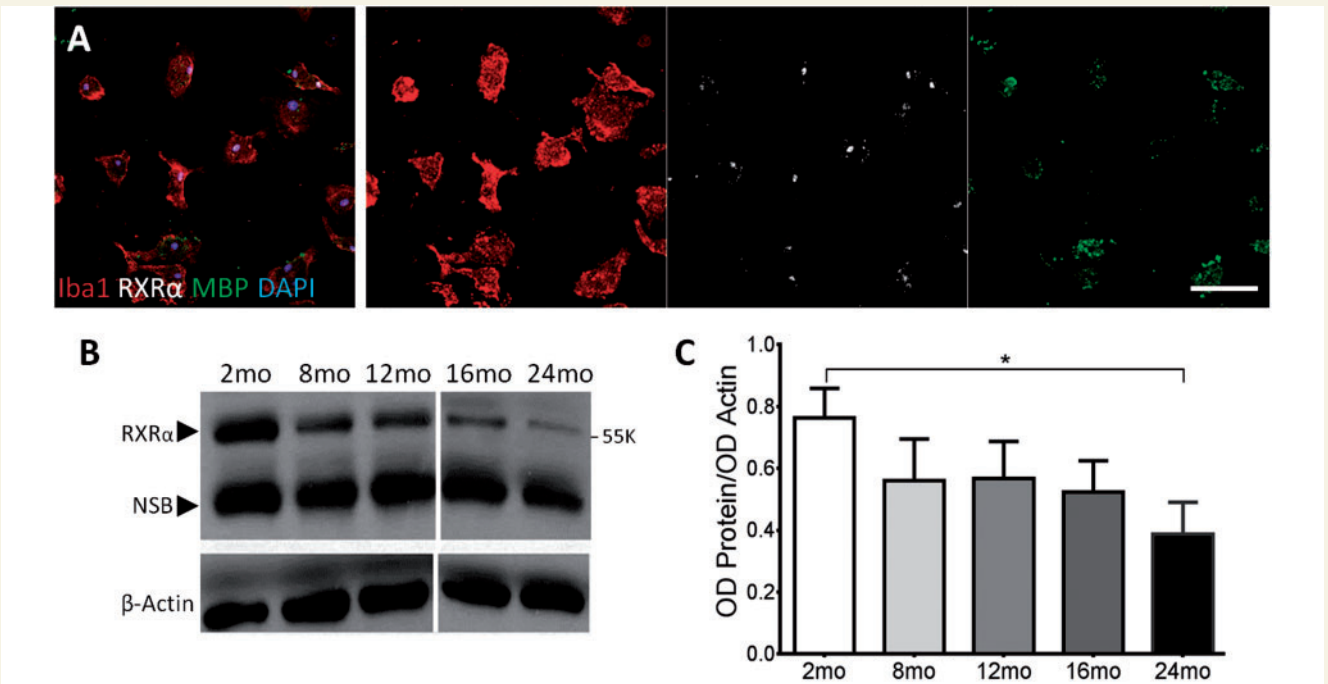

Figure 3 Myelin-phagocytosing macrophages undergo an age-related decline in RXRα expression. (**A**) Confocal analysis of Iba1$^+$ cells revealed nuclear localization of active RXRα in myelin-phagocytosing macrophages. Scale bar = 50 μm. (**B**) Levels of RXRα expression in macrophages derived from 2–24-month-old (mo) mice were determined by western blot and analysed by ImageJ. Dividing line indicates different gels. RXRα band is indicated at 55 K, with non-specific bands (NSB) at lower values indicated on the gel. (**C**) There was a significant reduction in RXRα expression in macrophages between 2- and 24-month-old mice. One-way ANOVA and *post hoc* Tukey's multiple comparisons test, mean ± SEM, $*P < 0.05$, n = 3/age group.

Figure 2 Continued

fluorescence intensity of resting monocytes). (**D** and **E**) Ingenuity Pathway Analysis of microarray results showed that RXR-related genes with significant fold changes ($P < 0.05$, $|FC| > 1.5$) were more highly upregulated in (**D**) young phagocytosing compared to (**E**) old phagocytosing groups. Blue = upregulated; yellow = downregulated. n = 3/group. (**F**) Quantitative PCR was performed using a Retinoic Acid Signaling RT2 Profiler PCR Array (SABiosciences) to confirm microarray results. Expression changes were calculated by comparing young or old phagocytosing cells to resting controls. Genes in the RXR pathway with $|FC| > 1.5$ are shown here, with RXR-related genes more upregulated in young phagocytosing monocytes. White bars = young cells versus resting; black bars = old cells versus resting. Two-way ANOVA and *post hoc* Bonferroni's correction, mean ± SEM, $*P < 0.05$, n = 6/group.

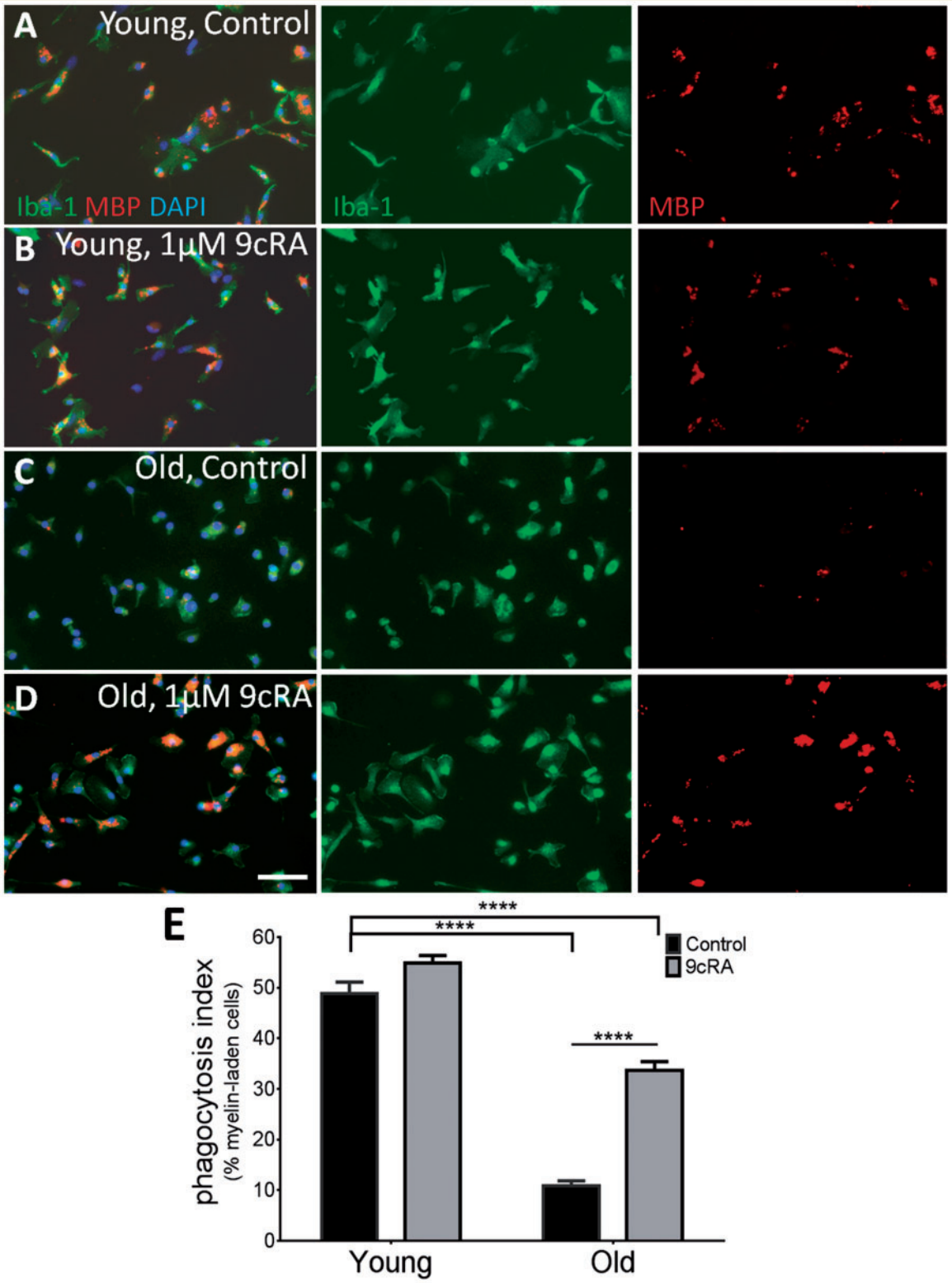

Figure 4 RXR agonist 9cRA stimulates myelin debris phagocytosis in aged macrophages. (**A** and **B**) Macrophages from 2-month-old mice are able to effectively consume myelin debris, both before (**A**, 48.9% ± 2.6%) and after treatment with 9cRA (**B**, 54.9% ± 1.5%). (**C**) However, 32-month-old senescent macrophages were not able to efficiently phagocytose debris. (**D** and **E**) Adding 1 μM 9cRA significantly increased myelin debris consumption in aged macrophages. More than half of young macrophages were able to effectively clear myelin, while only 10.9% (±1%) of old macrophages were able to; however, 9cRA significantly increased myelin clearance to 33.6% (±1.7%) in aged cells. Phagocytosis index = % $Myelin^+Iba^+$ cells. Scale bar = 50 μm. Two-way ANOVA and *post hoc* Sidak's multiple comparisons test, mean ± SEM, ****$P < 0.0001$, $n = 6$/age group.

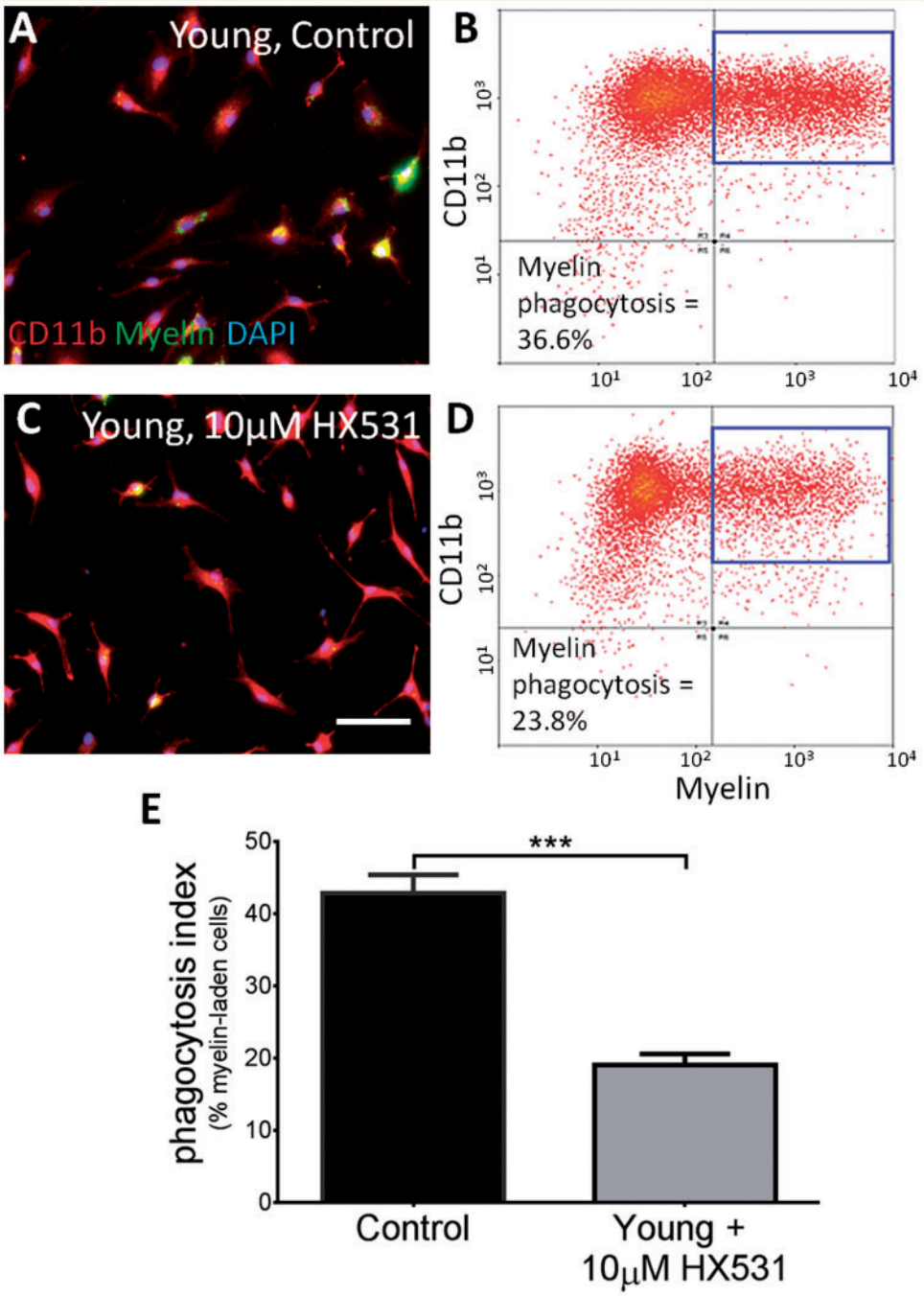

Figure 5 Loss of RXR function in young macrophages reduces myelin debris uptake *in vitro*. (**A–D**) DiO-labelled myelin was used to measure myelin debris clearance by immunocytochemistry and flow cytometry in young macrophages (**A** and **B**) and young macrophages treated with a synthetic RXR antagonist, HX531 (**C** and **D**). (**E**) Blocking RXR with 10 μM HX531 significantly reduced myelin debris uptake in young bone marrow monocyte-derived macrophages from 42.8% (±2.5%) in young controls to 19.06% (±1.5%) in HX531-treated cells. Phagocytosis index = % myelin$^+$CD11b$^+$ cells. Scale bar = 50 μm. Student's *t*-test, mean ± SEM, ***$P < 0.001$, $n = 4$/treatment.

constitutive RXR activation (Nagpal *et al.*, 1993; Laursen *et al.*, 2012) may be one of the key differences between young and old cells. The synthetic antagonist for RXR, HX531, was used to block RXR and determine if RXR activation was necessary for efficient myelin debris phagocytosis in young bone marrow monocyte-derived macrophages. Myelin$^+$/CD11b$^+$ cells were quantified by immunocytochemistry and flow cytometry. Young cells efficiently phagocytosed the DiO-labelled myelin (Fig. 5A and B), while macrophages treated with 10 μM HX531 showed reduced myelin debris uptake and significantly fewer double positive cells (Fig. 5C–E). Additionally, bone

marrow monocyte-derived macrophages from RXRα knockout mice displayed reduced myelin debris uptake compared to wild-type, which was not modifiable by activation of the RXR pathway (Supplementary Fig. 2), further demonstrating that when RXR activation is inhibited, myelin debris phagocytosis is significantly impaired in young bone marrow monocyte-derived macrophages. Thus, the RXR pathway seems necessary for efficient myelin debris phagocytosis in young macrophages.

To confirm the need for RXR activity in myelin debris phagocytosis *in vivo*, a LysM Cre-RXRα floxed system was used to knockout RXRα from myeloid cells in young mice. As this isoform of the receptor shows the highest expression in macrophage cell types (Roszer *et al.*, 2013), it was predicted to have the greatest effect. Mice were generated as previously described (Ricote *et al.*, 2006; Núñez *et al.*, 2010) by crossing LysM-Cre mice with RXRα floxed mice, resulting in macrophage-specific RXRα knockouts. Lysolecithin-induced focal demyelination was performed in 4-month-old wild-type and knockout mice. Oil Red O neutral lipid labelling was used to measure myelin debris. At 5 days post lesion induction, when oligodendrocyte progenitor cell recruitment into the lesion is maximal (Arnett *et al.*, 2004), there was little Oil Red O staining in the wild-type, but significantly more diffuse staining in the knockout (Fig. 6A, B and G), indicating reduced myelin debris clearance in the knockout at 5 days post lesion. Myelin debris clearance was more advanced at 14 days post lesion (Fig. 6C and D) and 21 days post lesion (Fig. 6E and F) in both the wild-type and knockout mice, with the staining being more punctate and consistent with intracellular staining of phagocytosed myelin (Kotter *et al.*, 2005), as compared to the more diffuse staining of extracellular myelin seen in 5 days post lesion knockouts. Recruitment of Iba1$^+$ macrophages to the lesion was not affected at any time point (Supplementary Fig. 3), signifying a reduced phagocytic efficiency in macrophages, and not reduced recruitment of myeloid cells.

As myelin debris contains inhibitors of oligodendrocyte progenitor cell differentiation (Kotter *et al.*, 2006; Baer *et al.*, 2009; Syed *et al.*, 2011), we hypothesized that the delay in myelin debris clearance in RXRα knockout mice would result in delayed remyelination. To assess remyelination in the absence of macrophage RXRα, several oligodendrocyte lineage and myelination markers were used: OLIG2 is a marker for all stages of the oligodendrocyte lineage; CC1 (encoded by *RB1CC1*) and PLP are markers of differentiated oligodendrocytes. We determined the density of CC1$^+$/OLIG2$^+$ mature oligodendrocytes in RXRα wild-type and knockout lesions at 5, 14, and 21 days post lesion (Fig. 6H and I). There was a significantly lower number of CC1$^+$/OLIG2$^+$ cells in the knockout at 14 days post lesion (Fig. 6I and J), suggesting delayed oligodendrocyte progenitor cell differentiation in the myeloid-specific knockout. This delay in oligodendrocyte progenitor cell differentiation had recovered by 21 days post lesion, where there was no significant difference in CC1$^+$ cells between wild-type and knockout (Fig. 6J). At 14 days post lesion, CC1$^-$/OLIG2$^+$ cells, likely representing oligodendrocyte progenitor cells, were more prevalent in knockout lesions than in wild-type (Fig. 6K). Again, the number of oligodendrocyte progenitor cells in the knockout was reduced by 21 days post lesion and was not significantly different from wild-type. *In situ* hybridization for the myelinating marker PLP was performed at 14 and 21 days post lesion (Fig. 6L and M). The delay in oligodendrocyte progenitor cell differentiation was confirmed in this experiment with fewer myelinating oligodendrocytes in the knockout at 14 days post lesion, indicating delayed remyelination (Fig. 6N). This impairment had again recovered by 21 days post lesion, when there was no significant difference in PLP$^+$ cell numbers between wild-type and knockout. The uninhibited oligodendrocyte progenitor cell recruitment and slowed differentiation (Fig. 6H–J) mimic the state in many chronically demyelinated multiple sclerosis lesions, where oligodendrocyte progenitor cells are recruited but fail to differentiate into myelinating oligodendrocytes (Wolswijk, 1998; Chang *et al.*, 2002). The delay in oligodendrocyte differentiation in knockouts was also associated with significantly thinner myelin sheaths (a higher g-ratio) compared to wild-type at 14 days post lesion (Fig. 6O–Q), shown by electron microscopy of demyelinated areas. The lower g-ratio in wild-type, calculated as the ratio of the myelinated axon diameter to the axon diameter, suggests a larger number of remyelinated axons in the wild-type at 14 days post lesion, consistent with Fig. 6J and N. Together, these findings indicate that RXRα plays an important role in efficient myelin debris clearance and rapid CNS remyelination.

Bexarotene reverses the age-related decline in RXR and myelin debris phagocytosis in human monocytes

Bexarotene is the only FDA-approved rexinoid (RXR agonist) currently available (Henney, 2000). Based on the significant effects of modulating this pathway in the murine system, we next determined the effects of this RXR agonist on myelin-phagocytosing human monocytes. Monocytes were isolated from young ($\leqslant 35$ years old) and old ($\geqslant 55$ years old) healthy volunteers and patients with multiple sclerosis. These cells were then treated with 1 μM bexarotene and exposed to FITC$^+$ pHrodo-labelled myelin. As in the initial experiment, the statistician first performed a sample size estimate on pilot data. After obtaining the predetermined number of volunteers per group, we observed that bexarotene treatment exerted a modest increase in myelin phagocytosis in monocytes derived from old healthy volunteers, which did not reach statistical significance. Similar to bone marrow monocyte-derived macrophages, treatment had no effect on myelin phagocytosis of young monocytes (Fig. 7A and C). Next, we studied monocytes derived from multiple sclerosis patients and found them to

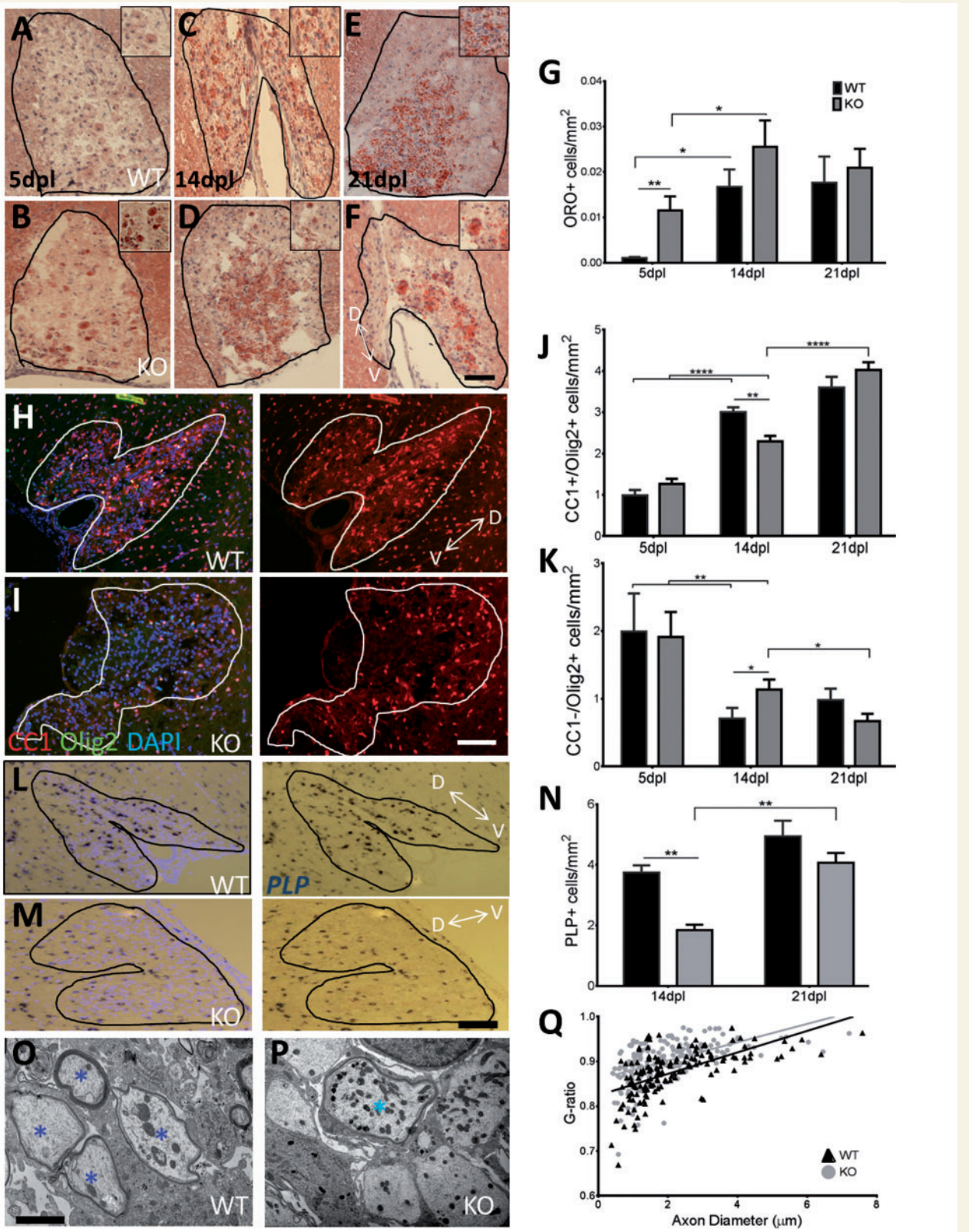

Figure 6 Macrophage-specific RXRα knockouts experience slowed myelin debris clearance, reduced oligodendrocyte progenitor cell differentiation, and delayed remyelination. (**A–F**) Oil red O was used to label neutral lipids in demyelinated lesions of RXRα myeloid-specific knockouts at 5 (**A** and **B**), 14 (**C** and **D**), and 21 days post lesion (**E** and **F**); enlarged, myelin-laden cells are represented in the *top right* corner (**A–F**). (**G**) Myelin debris uptake was significantly slowed in knockouts at 5 days post lesion. At 14 and 21 days post lesion, there is an increase in intracellular lipids, consistent with previous studies (Kotter *et al*., 2005). (**H** and **I**) CC1 labels mature oligodendrocytes and DAPI denotes the demyelinated lesion. (**J**) At 14 days post lesion, there is a significant decrease in $CC1^+/OLIG2^+$ mature oligodendrocytes in

(continued)

have uniformly decreased myelin phagocytosis compared to young healthy volunteers, with no clear correlation with age (Fig. 7 B, C and data not shown). Phagocytosis was also measured in monocytes and polarized macrophages from patients with multiple sclerosis, with impaired myelin debris phagocytosis in both cell types compared to young healthy volunteers (Fig. 7B and Supplementary Fig. 4). Bexarotene-enhanced myelin phagocytosis in healthy volunteer monocytes and significantly increased myelin debris phagocytosis in monocytes from multiple sclerosis patients (Fig. 7C), suggesting that RXR activation may significantly enhance myelin debris clearance in multiple sclerosis.

As bexarotene had a significant functional effect on patient-derived cells, we performed microarrays to ascertain the effects of bexarotene on monocytes from patients. Bexarotene treatment significantly increased the expression of several genes in the RXR pathway (shown in green) and significantly decreased expression of negative regulators of RXR (shown in red). The treatment affected four groups of RXR-related genes: RXR activators, nuclear binding partners of RXR, other binding partners of RXR, and RXR inhibitors (Fig. 7D). Of the genes with altered expression in patient monocytes on bexarotene treatment, 10 genes were found to play roles in inducing patient monocytes to behave more like healthy controls (Fig. 7E). For example, genes such as *EDN1*, *CXCL3*, and *CXCL1* are more highly expressed in multiple sclerosis patient monocytes compared to young healthy volunteers. However, when patient monocytes were treated with bexarotene, the expression of these genes decreased to levels similar to those seen in young healthy volunteers, whereas untreated patient monocytes behaved more similar to old healthy volunteer monocytes in RXR signalling (Supplementary Fig. 5). Thus, the gene profiles of patient monocytes became more similar to the profiles of efficiently phagocytosing healthy controls. This result further suggests that bexarotene treatment is able to create a healthier, more youthful state in human myelin-phagocytosing monocytes via activation of the RXR pathway.

Discussion

The aim of this study was to identify differences between young and old myelin-phagocytosing myeloid cells to identify therapeutically-modifiable pathway(s) that enhance myelin debris clearance and therefore potentially enhance remyelination in aged subjects with demyelinating disorders. By using multiple complementary assays, we identified systemic differences in the RXR pathway between efficiently-phagocytosing young and poorly-phagocytosing old monocytes/macrophages in mice and humans. We further demonstrated the link between the efficiency of myelin debris phagocytosis by cells of the myeloid lineage and the speed of remyelination in an experimental model of focal demyelination.

Myelin debris clearance is mediated by an innate immune response performed by both monocyte-derived macrophages and microglia. Microglia are derived from the yolk sac during early development and reside in the CNS through adulthood, whereas blood-derived monocytes are differentiated from bone marrow cells and are recruited to the CNS in response to an insult (Neumann *et al.*, 2009; Ginhoux *et al.*, 2010; Ousman and Kubes, 2012). These cells are difficult to distinguish once they are activated, but studies have suggested that monocyte-derived macrophages play a pivotal role in myelin debris clearance and CNS remyelination (Kotter *et al.*, 2005; Ruckh *et al.*, 2012), although both cell types become phagocytic macrophages (Neumann *et al.*, 2009; Olah *et al.*, 2012; Yamasaki *et al.*, 2014; Lampron *et al.*, 2015). Our results from *in vitro* studies support the notion that both cell types are able to phagocytose debris, with monocyte-derived cells showing greater phagocytosis (Fig. 1). In addition, the RXRα knockout used here was under control of the LysM-Cre, which shows little recombination in microglia (Goldmann *et al.*, 2013), indicating the delayed myelin debris clearance seen in knockouts is mainly due to RXR impairment in recruited myeloid cells. A particular focus was on monocytes, shown to be differentially regulated in young remyelinating and old remyelinating lesions (Ruckh, *et al.*, 2012). In human studies, we used freshly isolated *ex vivo* monocytes as a model, which uses minimal *in vitro* manipulations that may introduce non-physiological changes. Because of ease of recruitment of blood-derived monocytes to inflammatory multiple sclerosis lesions and proportional dominance of such myeloid cells in acutely demyelinating lesions (Hill *et al.*, 2004; Chuluundorj *et al.*, 2014; Ciccarelli *et al.*, 2014), we consider this model to be relevant to human disease. We confirmed our conclusions that patients with multiple sclerosis have a defect in myelin phagocytosis in undifferentiated

Figure 6 Continued

LysM-RXRα knockouts with an increase in $CC1^+$ cells at 21 days post lesion in the knockouts, indicating slowed differentiation. (**K**) There are also significantly more oligodendrocyte progenitor cells ($CC1^-/OLIG2^+$ cells) in the knockout at 14 days post lesion. (**L** and **M**) *In situ* hybridization of *PLP* in wild-type and knockout lesions at 14 days post lesion. (**N**) Myelinating oligodendrocytes were decreased in knockouts at 14 days post lesion. Scale bars = 100 μm. Two-way ANOVA and *post hoc* Tukey's multiple comparisons test, mean ± SEM, $^*P < 0.05$, $^{**}P < 0.01$, n = 4/time point. D↔V represents dorsal–ventral axis. (**O–Q**) Electron micrographs of demyelinated lesion tissue confirmed that (**Q**) knockouts have a higher g-ratio (Mean = 0.901 ± 0.024) than wild-type (mean = 0.875 ± 0.026) and less remyelination at 14 days post lesion. The scatterplot displays g-ratios as a function of axonal diameter (black = wild-type; grey = knockout). *Remyelinated axons. Scale bar = 2 μm. Student's *t*-test, $^{****}P < 0.0001$, n = 4/timepoint. WT = wild-type; KO = knockout.

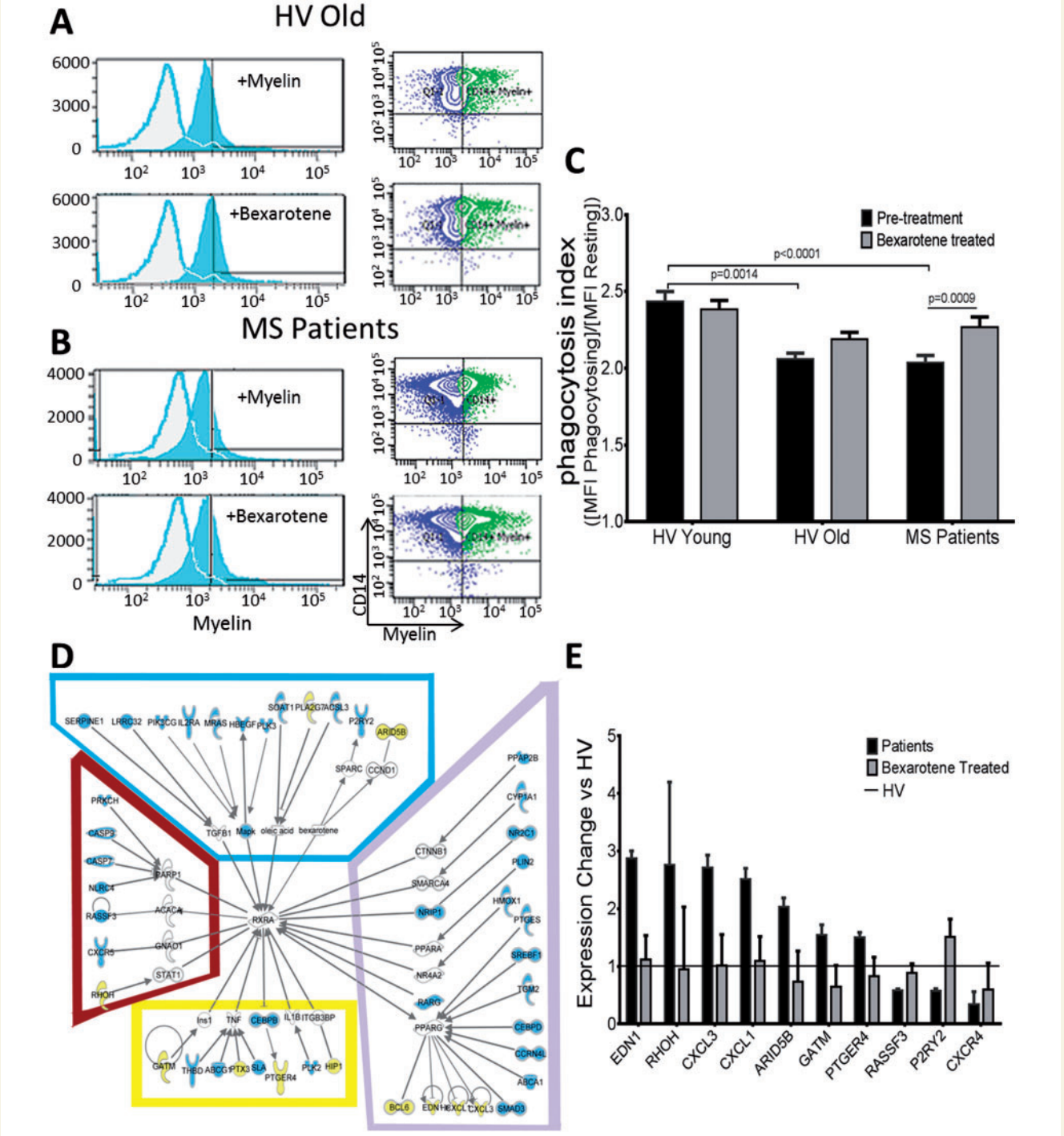

Figure 7 Bexarotene increases myelin debris phagocytosis and activates the RXR pathway in multiple sclerosis patient monocytes. (**A**) Monocytes from aged healthy volunteers (HV, $\geqslant$55 years old) show marginally improved myelin debris phagocytosis by adding 1 μM Bexarotene (not significant, 2.18 $\pm$ 0.04). n = 36/group. (**B**) Monocytes from progressive patients show a significant decrease compared to young healthy volunteers (2.10 $\pm$ 0.09); they also show a statistically significant improvement in myelin debris phagocytosis upon bexarotene treatment (2.24 $\pm$ 0.07). $P < 0.0009$, $n \geqslant 36$/group. (**C**) However, both treated and untreated aged and patient monocytes phagocytose myelin debris significantly less efficiently than young healthy volunteers (2.44 $\pm$ 0.06, $P < 0.0001$), which are not significantly affected by treatment (2.38 $\pm$ 0.05). Adjusted P-values for pairwise comparisons in a two-way repeated measures ANOVA with Tukey's procedure based on log-transformed outcomes, mean $\pm$ SEM. Data also presented in Fig. 2C. (**D**) Ingenuity Pathway Analysis was used to analyse microarrays comparing patient monocytes to bexarotene-treated monocytes. Several RXR-related genes are upregulated with treatment, shown here by pathway analysis. Blue box = RXR activators; purple box = nuclear receptor binding partners; yellow box = RXR inhibitors; brown box = other binding partners. (**E**) On bexarotene treatment, 10 genes had significant fold changes ($P < 0.05$) and expression profiles more like healthy volunteers (healthy volunteer = 1) compared to patient monocytes. Two-way ANOVA under false discovery rate multiple comparison correction and *post hoc* Tukey's honest significant difference test; n = 4/group.

monocytes as well as in M1 versus M2 differentiated macrophages. Previous literature shows that microglia and macrophages display a more pro-inflammatory M1 phenotype in old cells and more anti-inflammatory M2 in young (Lumeng *et al.*, 2011; Fenn *et al.*, 2012; Lee *et al.*, 2013; Ma *et al.*, 2015), and the spectrum of M1/M2 profiles are also differentially regulated in multiple sclerosis and may affect beneficial functions of monocytes (Vogel *et al.*, 2013), further suggesting modulating macrophage expression profiles, regulated through pathways such as RXR, is important for efficient phagocytosis.

RXR belongs to a family of nuclear receptors that act as both ligand-activated receptors and transcription factors for several downstream genes, including genes associated with immunoregulatory functions in monocytes and macrophages as well as genes associated with cholesterol transport (Repa *et al.*, 2000; Nagy and Schwabe, 2004; Daniel *et al.*, 2014). Three different genes (*RXRA*, *RXRB* and *RXRG*, encoding RXR-α, β and γ, respectively) and multiple splicing variants constitute the RXR family in vertebrates, and 9cRA is its natural ligand (Mangelsdorf *et al.*, 1992; Chen and Privalsky, 1995). As RXR is downregulated with ageing, activating the receptor may not only enhance activation of RXR but also increase RXR expression in aged cells because RXR has previously been shown to act as a transcription factor for its own expression as well as for other nuclear receptors (Baker, 2011; Dave, 2012; Evans and Mangelsdorf, 2014). In young monocytes and macrophages, activation of RXR does not have a functional effect on myelin phagocytosis. We hypothesize that this is because young cells can optimally phagocytose myelin debris, therefore further activating RXR does not affect function in these efficiently phagocytosing cells. In addition, RXR and its binding partners have previously been shown to display constitutive, ligand-independent activation (Nagpal *et al.*, 1993; Laursen *et al.*, 2012), which may be the case in young cells and not in old.

RXR can form homodimers but also acts as a binding partner for several other nuclear hormone receptors, such as the all-trans Retinoic acid receptor (RAR), thyroid hormone receptor, vitamin D receptor, peroxisome proliferator-activated receptors (PPAR) and Liver X Receptors (LXR). In resulting permissive heterodimers, such as PPAR and LXR, both RXR and its binding partner can bind their cognate ligands and cause ligand-dependent trans-activation. Moreover, each heterodimer has different DNA-binding specificity, resulting in the expression of genes downstream of both RXR and its permissive binding partner (Evans and Mangelsdorf, 2014). Genes shown to be significantly upregulated by activation of RXR and its binding partners (Fig. 7D and E) have also been involved in differentiation of oligodendrocytes and point toward other beneficial roles of myeloid cells in remyelination, such as releasing growth factors that promote remyelination. RXR activation increased expression of TGFB1 and HBEGF, known to enhance oligodendrocyte progenitor cell differentiation (McKinnon *et al.*, 1993; Scafidi *et al.*, 2014) and decreased expression of EDN1, CXCL1, and CXCL3, inflammatory molecules that impair oligodendrocyte progenitor cell differentiation (Hammond *et al.*, 2014).

Due to this combinatorial heterodimerization, RXR pathways have far-reaching effects in different cell types. For example, in a previous study we identified RXRγ as highly expressed during oligodendrocyte progenitor cell differentiation. Treatment with an RXR ligand improved remyelination in aged rats in this study (Huang *et al.*, 2011), making the RXR pathway of particular interest due to its reversible age-dependent role in both myelin debris phagocytosis and oligodendrocyte progenitor cell differentiation. Furthermore, macrophage-specific knockouts of RXRα in mice resulted in impaired clearance of apoptotic cells in a model of autoimmune kidney disease (Roszer *et al.*, 2011), and bexarotene, a clinically approved RXR agonist, increased clearance of amyloid deposits in an animal model of Alzheimer's disease (Cramer *et al.*, 2012). Both of these studies support the conclusion derived from the current paper, that RXR plays a role in phagocytosis in general and in myelin-debris clearance in particular. Bexarotene added in concentrations achievable *in vivo* with current dosing regimen, restored multiple sclerosis patient monocytes to the phagocytic efficiency seen in young healthy volunteers. The significant changes in phagocytosis seen in patients with multiple sclerosis may have an important functional consequence. As biological processes are time-dependent, minor changes in kinetics may have dramatic consequences for the outcome, as previously seen in systemic lupus erythematosus, where similarly mild but nevertheless significant defects in phagocytosis of apoptotic cells in patients was sufficient to induce immune responses against intracellular antigens (Herrmann, *et al.*, 1998; Fossati-Jimack *et al.*, 2013; Majai *et al.*, 2014).

We find it intriguing that RXR binding partners have likewise been implicated in the multiple sclerosis disease process, and future studies of the synergistic and specific activation of RXR and one of these binding partners in myeloid cells may prove to fully reverse deficiencies in myelin debris phagocytosis. Particular receptors in this regard include the PPARs (shown to have immunoregulatory functions in macrophages and potentially in multiple sclerosis; Odegaard *et al.*, 2007; Drew *et al.*, 2008), LXRs (shown to be activated by fatty acids present in myelin debris; Bogie *et al.*, 2012), as well as roles in modulation of phagocytosis and pro- and anti-inflammatory functions of macrophages through RAR, TR, and VDR (Glass and Saijo, 2010; Nagy *et al.*, 2012). The role of thyroid hormone in differentiation and the epidemiological link between vitamin D deficiency and risk for development of multiple sclerosis (Ascherio *et al.*, 2014) further strengthen our conclusions and suggest that modulating RXR pathways may influence the multiple sclerosis disease process. We have demonstrated that bexarotene reverses functional defects in myelin phagocytosis by multiple sclerosis monocytes, while changing their expression profile to a more 'youthful' state. The current availability of bexarotene

makes a proof of principle clinical trial in human subjects with multiple sclerosis feasible as well as appropriate and much will be learned about the extent and management of side-effects from an analogous study currently ongoing for Alzheimer's disease (Clinicaltrials.gov identifier NCT01782742).

Acknowledgements

We thank Dr Abdel Elkalhoun and WeiWei Wu for Microarray assistance, Dr Daniel Morrison for Electron Microscopy, and Chris McMurran for confocal imaging. The authors have no conflicting financial interests.

Funding

This work was supported by grants from the UK Multiple Sclerosis Society, Wellcome-Trust, NINDS/NIH Intramural Research Program, Health Research Board Scholars Program, Gates-Cambridge Scholarship, and Spanish Ministry of Economy and Competitiveness (SAF2012-31483).

Supplementary material

Supplementary material is available at *Brain* online.

References

Arnett HA, Fancy SP, Alberta JA, Zhao C, Plant SR, Kaing S, et al. bHLH transcription factor Olig1 is required to repair demyelinated lesions in the CNS. Science 2004; 306: 2111–15.

Ascherio A, Munger KL, White R, Kochert K, Simon KC, Polman CH, et al. Vitamin D as an early predictor of multiple sclerosis activity and progression. JAMA Neurol 2014; 71: 306–14.

Baer AS, Syed YA, Kang SU, Mitteregger D, Vig R, ffrench-Constant C, et al. Myelin-mediated inhibition of oligodendrocyte precursor differentiation can be overcome by pharmacological modulation of Fyn-RhoA and protein kinase C signalling. Brain 2009; 132: 465–81.

Baker ME. Origin and diversification of steroids: co-evolution of enzymes and nuclear receptors. Mol Cell Endocrinol 2011; 334: 14–20.

Bogie JF, Timmermans S, Huynh-Thu VA, Irrthum A, Smeets HJ, Gustafsson JA, et al. Myelin-derived lipids modulate macrophage activity by liver X receptor activation. PLoS One 2012; 7: e44998.

Chang A, Tourtellotte WW, Rudick R, Trapp BD. Premyelinating oligodendrocytes in chronic lesions of Multiple sclerosis. NEJM 2002; 346: 165–73.

Chari DM, Crang AJ, Blakemore WF. Decline in rate of colonization of oligodendrocyte progenitor cell (OPC)-depleted tissue by adult OPCs with age. J Neuropath Exp Neur 2003; 62: 908–16.

Chen H, Privalsky ML. Cooperative formation of high-order oligomers by retinoid X receptors: an unexpected mode of DNA recognition. PNAS 1995; 92: 422–6.

Chuluundorj D, Harding SA, Abernathy D, la Flamme AC. Expansion and preferential activation of the CD14 + CD16 + monocyte subset during multiple sclerosis. Immun Cell Biol 2014; 92: 509–17.

Ciccarelli O, Barkhof F, Bodini D, Stefano N, Golay X, Nicolay K, et al. Pathogenesis of multiple sclerosis: insights from molecular and metabolic imaging. Lancet Neurol 2014; 13: 807–22.

Cramer PE, Cirrito JR, Wesson DW, Lee CY, Karlo JC, Zinn AE, et al. ApoE-directed therapeutics rapidly clear beta-amyloid and reverse deficits in AD mouse models. Science 2012; 335: 1503–6.

Daniel B, Nagy G, Hah N, Horvath A, Czimmerer Z, Poliska S, et al. The active enhancer network operated by liganded RXR supports angiogenic activity in macrophages. Gene Dev 2014; 28: 1562–77.

Dave V, Kaul, D, Sharma, M. Crosstalk between RXR, LXR and VDR within blood mononuclear cellular model. Indian J Exp Biol 2012; 50: 35–40.

Drew PD, Xu J, Racke MK. PPAR-gamma: therapeutic potential for multiple sclerosis. PPAR Res 2008; 2008: 627463.

Evans RM, Mangelsdorf DJ. Nuclear receptors, RXR, and the big bang. Cell 2014; 157: 255–66.

Fancy SPJ, Zhao C, Franklin RJM. Increased expression of Nkx2.2 and Olig2 identifies reactive oligodendrocyte progenitor cells responding to demyelination in the adult CNS. Mol Cell Neurosci 2004; 27: 247–54.

Fenn AM, Henry CJ, Huang Y, Dugan A, Godbout JP. Lipopolysaccharide-induced interleukin (IL)-4 receptor-a expression and corresponding sensitivty to the M2 promoting effects of IL-4 are impaired in microglia of aged mice. Brain Behav Immun 2012; 26: 766–77.

Fossati-Jimack L, Ling GS, Cortini A, Szajna M, Malik TH, McDonald JU, et al. Phagocytosis is the main CR3-mediated function affected by the lupus-associated variant of CD11b in human myeloid cells. PloS One 2013; 8: e57082.

Franklin RJM, ffrench-Constant C. Remyelination in the CNS: from biology to therapy. Nat Rev Neurosci 2008; 9: 839–55.

Franklin RJM, Gallo V. The translational biology of remyelination: past, present, and future. Glia 2014; 62: 1905–15.

Ginhoux F, Greter M, Leboeuf M, Nandi S, See P, Gokhan S, et al. Fate mapping analysis reveals that adult microglia derive from primitive macrophages. Science 2010; 330: 841–45.

Glass, CK, and Saijo K. Nuclear receptor transrepression pathways that regulate inflammation in macrophages and T cells. Nat Rev Immun 2010; 10: 365–76.

Goldmann T, Wieghofer P, Muller PF, Wolf Y, Varol D, Yona S, et al. A new type of microglia gene targeting shows TAK1 to be pivotal in CNS autoimmune inflammation. Nat Neurosci 2013; 16: 1618–26.

Goldschmidt T, Antel J, Konig FB, Bruck W, Kuhlmann T. Remyelination capacity of the MS brain decreases with disease chronicity. Neurology 2009; 72: 1914–21.

Hammond TR, Gadea A, Dupree J, Kerninon C, Nait-Oumesmar B, Aguirre A, et al. Astrocyte-derived endothelin-1 inhibits remyelination through notch activation. Neuron 2014; 81: 588–602.

Henney JE. From the food and drug administration. JAMA 2000; 283: 1131.

Herrmann M, Voll RE, Zoller OM, Hagenhofer M, Ponner BB, Kalden JR Impaired phagocytosis of apoptotic cell material by monocyte-derived macrophages from patients with systemic lupus erythematosus. Arthritis Rheum 1998; 41: 1241–50.

Heyman RA, Mangelsdorf DJ, Dyck JA, Stein RB, Eichele G, Evans RM, et al. 9-cis retinoic acid is a high affinity ligand for the retinoid X receptor. Cell 1992; 68: 397–406.

Hill KE, Zollinger LV, Watt HE, Carlson NG, Rose JW. Inducible nitric oxide synthase in chronic active multiple sclerosis plaques: distribution, cellular expression and association with myelin damage. J Neuroimmun 2004; 151: 171–9.

Huang JK, Jarjour AA, Nait Oumesmar B, Kerninon C, Williams A, Krezel W, et al. Retinoid X receptor gamma signaling accelerates CNS remyelination. Nat Neurosci 2011; 14: 45–53.

Kotter MR, Li WW, Zhao C, Franklin RJM. Myelin impairs CNS remyelination by inhibiting oligodendrocyte precursor cell differentiation. J Neurosci 2006; 26: 328–32.

Kotter MR, Zhao C, van Rooijen N, Franklin RJM. Macrophage-depletion induced impairment of experimental CNS remyelination is associated with a reduced oligodendrocyte progenitor cell response and altered growth factor expression. Neurobiol Dis 2005; 18: 166–75.

Kuhla A, Blei T, Jaster R, Vollmar B. Aging is associated with a shift of fatty metabolism toward lipogenesis. J Gerontol A Biol 2011; 66A: 1192–200.

Lampron A, Larochelle A, Laflamme N, Prefontaine P, Plante MM, Sanchez MG, et al. Inefficient clearance of myelin debris by microglia impairs remyelinating processes. J Exp Med 2015; 212: 481–95.

Laursen KB, Wong P-M, Gudas LJ. Epigenetic regulation by RARα maintains ligand-independent transcriptional activity. Nucleic Acids Res 2012; 40: 102–15.

Lee DC, Ruiz CR, Lebson L, Selenica MB, Rizer J, Hunt JB, et al. Aging enhances classical activation but mitigates alternative activation in the central nervous system. Neuro Aging 2013; 34: 1610–20.

Levine JM, Reynolds R. Activation and proliferation of endogenous oligodendrocyte precursor cells during ethidium bromide-induced demyelination. Exp Neurol 1999; 160: 333–47.

Linehan E, Dombrowski Y, Snoddy R, Fallon PG, Kissenpfennig A, Fitzgerald DC. Ageing impairs peritoneal but not bone marrow-derived macrophage phagocytosis. Aging Cell 2014; 13: 699–708.

Lowe M, Plosker G. Bexarotene. Am J Clin Dermatol 2000; 1: 245–50.

Lumeng CN, Liu J, Geletka L, Delaney C, DelProposto J, Desai A, et al. Aging is associated with an increase in T cells and inflammatory macrophages in visceral adipose tissue. J Immunol 2011; 187: 6208–16.

Ma Y, Chiao YA, Clark R, Flynn ER, Yabluchanskiy A, Ghasemi O, et al. Deriving a cardiac ageing signature to reveal MMP-9-dependent inflammatory signalling in senescence. Cardiovasc Red 2015; 106: 421–31.

Majai G, Kiss E, Tarr T, Zahuczky G, Hartman Z, Szegedi G, et al. Decreased apopto-phagocytic gene expression in the macrophages of systemic lupus erythematosus patients. Lupus 2014; 23: 133–45.

Mangelsdorf DJ, Borgmeyer U, Heyman RA, Zhou JY, Ong ES, Oro AE, et al. Characterization of three RXR genes that mediate the action of 9-cis retinoic acid. Gene Dev 1992; 6: 329–44.

Mckinnon RD, Piras G, Ida JA, Dubois-Dalcq M. A role for TGF-beta in oligodendrocyte differentiation. J Cell Biol 1993; 121: 1397–407.

Menéndez-Gutiérrez MP, Rőszer T, Fuentes L, Núñez V, Escolano A, Redondo JM, et al. Retinoid X receptors orchestrate osteoclast differentiation and postnatal bone remodeling. J Clin Invest 2015; 125: 809–23.

Moyon S, Dubessy AL, Aigrot MS, Trotter M, Huang JK, Dauphinot L, et al. Demyelination causes adult CNS progenitors to revert to an immature state and express immune cues that support their migration. J Neurosci 2015; 35: 4–20.

Nagpal S, Friant S, Nakshatri H, Chambon P. RARs and RXRs: evidence for two autonomous transactivation functions (AF-1 and AF-2) and heterodimerization *in vivo*. EMBO 1993; 12: 2349–60.

Nagy L, Schwabe JW. Mechanism of the nuclear receptor molecular switch. Trends Biochem Sci 2004; 29: 317–24.

Nagy L, Szanto A, Szatmari I, Szeles L. Nuclear hormone receptors enable macrophages and dendritic cells to sense their lipid environment and shape their immune response. Physio Rev 2012; 92: 739–89.

Neumann H, Kotter MR, Franklin RJM. Debris clearance by microglia: an essential link between degeneration and regeneration. Brain 2009; 132: 288–95.

Núñez V, Alameda D, Rico D, Mota R, Gonzalo P, Cedenilla M, et al. Retinoid X receptor α controls innate inflammatory responses through the up-regulation of chemokine expression. PNAS 2010; 107: 10626–31.

Odegaard JI, Ricardo-Gonzalez RR, Goforth MH, Morel CR, Subramanian V, Mukundan L, et al. Macrophage-specific PPARgamma controls alternative activation and improves insulin resistance. Nature 2007; 447: 1116–20.

Olah M, Amor S, Brouwer N, Vinet J, Eggen B, Biber K, et al. Identification of a microglia phenotype supportive of remyelination. Glia 2012; 60: 306–21.

Ousman SS, Kubes P. Immune surveillance in the central nervous system. Nat Neurosci 2012; 15: 1096–101.

Repa JJ, Turley SD, Lobaccaro J-MA, Medina J, Li L, Lustig K, et al. Regulation of absorption and ABC1-mediated efflux of cholesterol by RXR heterodimers. Science 2000; 289: 1524–9.

Ricote M, Snyder CS, Leung H-Y, Chen J, Chien KR, Glass CK. Normal hematopoiesis after conditional targeting of RXRα in murine hematopoietic stem/progenitor cells. J Leukocyte Biol 2006; 80: 850–61.

Roszer T, Menendez-Gutierrez MP, Cedenilla M, Ricote M. Retinoid X receptors in macrophage biology. Trends Endocrin Met 2013; 24: 460–8.

Roszer T, Menendez-Gutierrez MP, Lefterova MI, Alameda D, Nunez V, Lazar MA, et al. Autoimmune kidney disease and impaired engulfment of apoptotic cells in mice with macrophage peroxisome proliferator-activated receptor gamma or retinoid X receptor alpha deficiency. J Immunol 2011; 186: 621–31.

Ruckh JM, Zhao JW, Shadrach JL, van Wijngaarden P, Rao TN, Wagers AJ, et al. Rejuvenation of regeneration in the ageing central nervous system. Cell Stem Cell 2012; 10: 96–103.

Scafidi, J, Hammond TR, Scafidi S, Ritter J, Jabonska B, Roncal M, et al. Intransal epidermal growth factor treatment rescues neonatal brain injury. Nature 2014; 506.7487: 230–4.

Schreiner L, Huber-Lang M, Weiss ME, Hohmann H, Schmolz M, Schneider EM. Phagocytosis and digestion of pH-sensitive fluorescent dye (Eos-FP) transfected E. coli in whole blood assays from patients with severe sepsis and septic shock. J Cell Comm Signal 2011; 5: 135–44.

Shen S, Sandoval J, Swiss VA, Li J, Dupree J, Franklin RJM, et al. Age-dependent epigenetic control of differentiation inhibitors is critical for remyelination efficiency. Nat Neurosci 2008; 11: 1024–34.

Shields SA, Gilson JM, Blakemore WF, Franklin RJM. Remyelination occurs as extensively but more slowly in old rats compared to young rats following gliotoxin-induced CNS demyelination. Glia 1999; 28: 77–83.

Sim FJ, Zhao C, Penderis J, Franklin RJM. The age-related decrease in CNS remyelination efficiency is attributable to an impairment of both oligodendrocyte progenitor recruitment and differentiation. J Neurosci 2002; 22: 2451–9.

Syed YA, Hand E, Mobius W, Zhao C, Hofer M, Nave KA, et al. Inhibition of CNS remyelination by the presence of semaphorin 3A. J Neurosci 2011; 31: 3719–28.

Vogel DYS, Vereyken EJF, Glim JE, Heijnen PDAM, Moeton M, van der Valk P, et al. Macrophages in inflammatory multiple sclerosis lesions have an intermediate activation status. J Neuroinflamm 2013; 10: 35.

Wolswijk, G. Chronic stage multiple sclerosis lesions contain a relatively quiescent population of oligodendrocyte precursor cells. J Neurosci 1998; 18: 601–9.

Woodruff RH, Fruttiger M, Richardson WD, Franklin RJM. Platelet-derived growth factor regulates oligodendrocyte progenitor numbers in adult CNS and their response following CNS demyelination. Mol Cell Neurosci 2004; 25: 252–62.

Yamasaki R, Lu H, Butovsky O, Ohno N, Rietsch AM, Cialic R, et al. Differential roles of microglia and monocytes in the inflamed central nervous system. J Exp Med 2014; 211: 1533–49.

Zawadzka M, Rivers LE, Fancy SP, Zhao C, Tripathi R, Jamen F, et al. CNS-resident glial progenitor/stem cells produce Schwann cells as well as oligodendrocytes during repair of CNS demyelination. Cell Stem Cell 2010; 6: 578–90.